BIBECHANA
A Multidisciplinary Journal of Science, Technology and Mathematics
ISSN 2091-0762 (Print), 2382-5340 (0nline)
Journal homepage: http://nepjol.info/index.php/BIBECHANA
Publisher: Research Council of Science and Technology, Biratnagar, Nepal

Study of ambient environment around Asymptotic Giant Branch Carbon Star: IRAS 01142+6306

L. Khanal[1], D. R. Upadhyay[1*], A.K. Jha[2], B. Aryal[2]
[1]Amrit Campus, Tribhuvan University, Thamel, Kathmandu Nepal.
[2]Central Department of Physics, Tribhuvan University, Kirtipur, Kathmandu, Nepal.
[*]Email: mnadphy03@gmail.com[*]

Article history: Received 01 May, 2018; Accepted 04 September, 2018
DOI: http://dx.doi.org/10.3126/bibechana.v16i0.20998

Abstract

We studied dust environment such as flux, temperature, mass and inclination angle of the cavity structure around the C-rich asymptotic giant branch star in 60 μm and 100 μm wavelengths band using Infrared Astronomical Survey. We observed the data of AGB star having IRAS name 01142+6306 corresponding to R.A.(J2000)= 01^h 17^m 33.504^s and Dec.(J2000)= 63^0 22' 4.98'. Flexible image transport system image was downloaded from Sky View Observatory; we obtained the surrounding flux density using software Aladinv2.5. The dust color average temperature and mass are found to be 25.08 K and 4.73×10^{26} kg (0.00024 $M_\odot$) respectively. The dust color temperature ranges from 18.76 ± 3.16 K to 33.21 ± 4.07 K. The isolated cavity like structure around AGB star has extension 45.67 parsec and contraction 17.02 parsec was observed using detailed calculation. The core region is found to be edge-on having inclination angle 79.46^o.

Keywords: ISM; AGB star; Dust color temperature; Dust mass; Inclination angle.

1. Introduction

The interstellar medium (ISM) is the low density matter space between star and surrounding. The ISM contains gas in molecular, atomic or ionic form as well as cosmic rays and dust particles. By mass, 99% is gas and 1 % is dust particle [1]. The percentage of gas particle is 91 % Hydrogen, 9 % are Helium and 0.1 % are the atoms of elements heavier than Hydrogen and Helium [2]. The most abundant component in ISM is Hydrogen and its various forms: Molecular form (H_2), Neutral form(HI) and ionized form (HII) [3]. ISM environment is slightly different around the Asymptotic Giant Branch (AGB) star as compared to main sequence stars. Stellar wind of AGB, Supergiant interactions with ISM, supernova explosion and releasing matter of planetary nebulae have major roles for the formation of dilute ISM. This thermally unstable star burns vigorously and certainly extinguishes. During thermal pulse He shell performs $10^7 L_\odot$ for short period and forms convective zones with releasing excessive mass and tremendous amount of energy. This approximate

composition of this zone is 25 % Carbon and 75% Helium. Out of this, AGB wind and supergiant interaction plays prominent role for the formation and interaction between ambient ISM and AGB star. During the stellar evolution, when the normal star terminates from the main sequence of HR diagram, star becomes more luminous and red in color. This stage is late stage of stellar evolution, which is generated by finishing Hydrogen (H) fuel and abundant central Helium(He) ash. The asymptotic star evolves when the mass of the star is (1-8) $M_{\odot}$ and is located at the right and upper part of HR diagram [4]. In this research work we discussed how mass is distributed around AGB star, dust color temperature distribution and cavity like structure gives wide range of area for studying the interaction between ISM and AGB star. Low and Intermediate Mass Star (LIMS) evolve and become Asymptotic Giant Branch stars: luminous ($L_{star}=10^4L_{\odot}$), cool (T_{eff} =3000K) giants (R_{star} =1 AU), which lose mass at high rates (10^{-7} to a few times $10^{-4}M_{\odot}$/yr) [5].

Aryal & Weinberger (2006) discovered a new isolated interstellar nebula (RA = 08^h27^m (J2000), Dec = +25°54' (J2000)) found at 60 μm and 100 μm on IRAS maps. It has dimensions of ~140' × 70' and a cone-like shape, suggesting interaction with ambient interstellar matter or external radiation field [6]. They used similar method for as we have using calculating dust color temperature and found that the southern nucleus is about 34±4 K temperature of its northern counterpart 32±4 K. The eastern filamentary structures are slightly cooler (20±2 K) than the western filamentary structures (26±3 K) [6]. Again similar work done by Jha et al.(2017) in KK loops and pulsar coordinates [7]. Here we have presented work related to asymptotic giant branch star by using similar methods. AGB stars are generally classified as Oxygen-rich (M-type) or Carbon-rich (C-type) based on the chemistry and composition of the photosphere and/or the outer envelope [5]. We have investigate the surrounding temperature, mass and cavity around the C-rich AGB star CGCS201 at a distance 4.49 kpc[8] and lies at galactic latitude 0.645^0 using IRAS survey [9]. We have uses method developed by Henning et. al. (1990) and Hildebrand et al.(1983) [10] data are obtained and cross checked from SkyView Virtual Observatory [10] and SIMBAD [11] respectively.

2. Material and Methods

Infrared Astronomical Satellite Survey (IRAS) mission performed very precise, sensitive of sky survey at 12 μm, 25 μm, 60 μm and 100 μm. The Infrared Astronomical Satellite (IRAS) mission was a combined effort and joint project by the United States (NASA), the Netherlands (NIVR), and the United Kingdom (SERC) [6]. This satellite configuration and survey were optimized for maximally reliable captures of point sources for ten months in 1983, IRAS captured more than 95%. Here most of the sky survey and images has been taken from SkyView Virtual observatory [9].

We scanned 12 μm, 25 μm, 60 μm, 100 μm IRAS survey using Virtual Sky View Observatory[10] to get the Flexible Image Transport System (FITS) image. When we enter the coordinate RA($01^h17^m33{:}504^s$) and Dec. ($+63^0$ 22' 4:98''), (Galactic Longitude/Latitude:$125.85^o/0.645^0$) [8]. The FITS image is capable of carrying the physical information (flux density) at our region of interest.

We tagged 225 pixels at 60 micron and 100 micron to get the relative flux density. The nature of contour depends upon whether the formation of cavity is isolated or not. Also the ambient pixels and tagging depends upon the probable location of our AGB star.

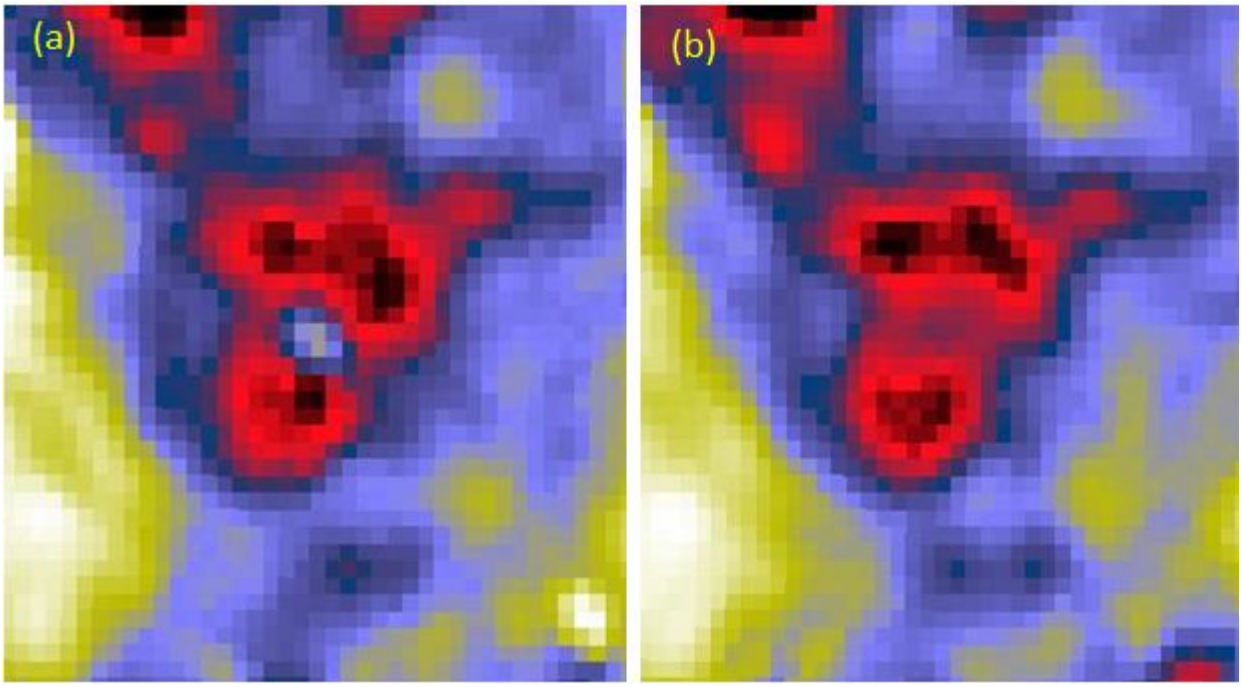

Fig. 1 : (a) and (b) IRAS 60 μm and 100 μm far infrared image around AGB star centered at R.A. (J2000) = $06^h\ 51^m\ 54.02^s$, Dec. (J2000) = $-01^0\ 35'\ 43''$[9] .

3. Theory

3. 1 Dust Color Temperature Estimation

The flux density of emission at a wavelength λ_i is given by Schnee et al. (2005) [12].

$$F_i = \left[\frac{2hc}{\frac{hc}{\lambda_i^3(e^{\frac{\lambda_i KT_d}{}}-1)}}\right] N_d \alpha \lambda_i^{-\beta} \Omega_i \qquad (1)$$

Where N_d represents column density of dust grains, α is a constant that relates the flux to the optical depth of the dust, β is the emissivity spectral index and Ω_i is the solid angle subtended at λ_i by the detector. Following [13], we use the equation

$$\beta = \frac{1}{\delta + \omega T_d} \qquad (2)$$

To describe the observed inverse relationship between termperature and emissivity spectral index. Here δ and ω are free parameters. Dupace et al. (2003)[13] found that the temperature dependence of the emissivity spectral index fits very well with the hyperbolic approximating function. Considering temperature as an independent variable, the best fit gives $\delta = 0.40 \pm 0.02$ and $\omega = 0.0079 \pm 0.0005 K^{-1}$, with the χ^2/degree of freedom=120/120. With the assumption that the dust emission is optically thin at 60 μm and 100 μm and $\Omega_{60} \cong \Omega_{100}$, we can write the ratio, R, of the flux densities at 60 μm and 100 μm as

$$R = 0.6^{-(3+\beta)} \left[\frac{e^{\frac{144}{T_d}}-1}{e^{\frac{240}{T_d}}-1}\right] \qquad (3)$$

Once the approximate value of β is known , one can use equation (3) to derive T_d. The value of β depends on such dust grain properties as composition, size and compactness. For reference, a pure blackbody would have β=0, the amorphous layer-lattice matter has $\beta \sim 1$ and the metals and crystalline dielectrics have $\beta \sim 2$[13].

For a smaller value of T_d, 1 can be dropped form both numerator and denominator of equation (3) and it takes the form

$$R = 0.6^{-(3+\beta)} \frac{e^{\frac{144}{T_d}}}{e^{\frac{240}{T_d}}} \quad (4)$$

To determine the dust color temperature we required the flux densities at 60 μm to 100 μm. The dust temperature T_d in each pixel of a FITS image can be obtained by assuming that the dust in a single beam is isothermal and that the observed ratio of 60 μm to 100 μm emission is due to black body radiation from dust grains at T_d, modified by a power law of spectral emissivity index.

Taking natural logarithm on both sides of equation (4), we find the expression used for the dust temperature estimation as [13],

$$T_d = \frac{-96}{\ln\left[R \times .06^{3+\beta}\right]} \quad (5)$$

where

$$R = \frac{F(60\mu m)}{F(100\mu m)} \quad (6)$$

Here F(60μm) and F(100μm) are the flux densities in 60 μm and 100 μm respectively [13].

3.2 Dust Mass Estimation

The dust masses are estimated from the IR flux densities. The resulting dust mass depends on the physical and chemical properties of the dust - grains. The dust masses are estimated using (Hildebrand 1983)[10];

$$M_{dust} = \frac{4}{3}\frac{a\rho}{Q_\nu}\left[\frac{F_\nu D^2}{B(\nu,T)}\right] \quad (7)$$

Where, a = Weighted grain size = 0.1 μm

ρ = Grain density= 3000 kgm^{-3}

Q_ν= grain emissivity = 0 .0010 for 100μm and 0.0046 for 60μm respectively [15].

F_ν = total flux density of the region whose mass is to be determined, $F_\nu = f \times 5.288 \times 10^{-9} MJy/sr$

D = distance of the structure

$B(\nu, T)$= Planck's function [10].

where, h = Planck's constant, c = velocity of light, ν = frequency at which the emission is observed & T= the average temperatures of the region.

Using values of different parameters equation (7) takes the form.

$$M_{dust} = 0.4\left[\frac{F_\nu D^2}{B(\nu,T)}\right] \quad (8)$$

The distance D and co-ordinate was taken from the source of catalogue paper [8].

We use the equation (8) for the calculation of the dust mass.

3.3 Inclination

Inclination angle is the angle between line of sight and the plane of celestial object projected in the sphere. Holmberg (1946) [16] established a simple model to find the inclination angle of celestial objects. Holmberg equation is the relation between the axial ratio (b/a) and the inclination angle (i), the angle between the line of sight and normal to the galactic plane. The flatness factor (q^*) = 0.33 is assumed by considering oblate spheroid. In this case, the equation of the ellipse can be written as

$$\frac{x^2}{a^2} + \frac{y^2}{a^2 q*^2} = 1 \quad (9)$$

The equation of the tangent at point P is

$$y = kx + y_0 \quad (10)$$

where, $k = tan(90 - i) = cot\, i$ and y-intercept OQ = y_o

Solving above equations, we get

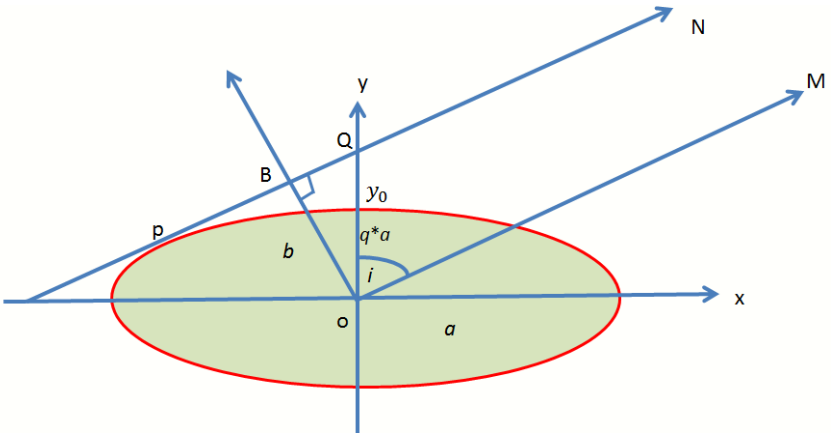

Fig. 2: A schematic representation of inclination angle. Here 'a' and 'q*a' represent the semi major and minor axes of ellipse.

$$x = \frac{-2y_0\,k \pm \sqrt{\{(2y_0k)^2 - 4(q*^2+k^2)(y_o^2 - q*^2a^2)\}}}{2(q*^2+k^2)} \tag{11}$$

The line touches the ellipse at only one point P, if $a^2k^2 + a^2q*^2$

From above figure, $sin\, i = \frac{b}{y_o}$

Using $y_o = \frac{b}{sini}$ and $k = cot\, i$, we get,

$$\cos^2 i = \frac{\frac{b^2}{a^2} - q*^2}{1 - q*^2} \tag{12}$$

is called 'Holmberg Formula' for inclination angle [16].

$$\therefore \text{Angle of inclination } (i) = \cos^{-1}\left(\sqrt{\frac{\frac{b^2}{a^2} - q*^2}{1 - q*^2}}\right) \tag{13}$$

4. Result and Discussion

4. 1 Flux Density Variation

The best fit line between F60 and F100 with error 0.02, slope of the linear fitted line is 0.28 whereas the coefficient of determination is 0.68. It gives average value of temperature nearly 25.08 K. Again coefficient of determination shows the square of the correlation between 100 μm flux density and 60 μm as shown in Fig. 3. It indicates inside the cavity region flux density data follows best fit condition nearly 68%. The slope of flux at 60 μm and 100 μm is calculated in equation (6). The nonlinear phenomenon is due to the rapid increase in flux at intersecting point between extension (AB) and contraction (CD) as shown in Fig.6.

We studied the contour map of flux density with respect to right ascension and declination as shown in Fig.4(b). The violet color represents the minimum flux and red color represents higher flux density region around AGB star. It has been observed that two cavity was formed by the central and dense flux region around carbon star : IRAS 01142+6306.

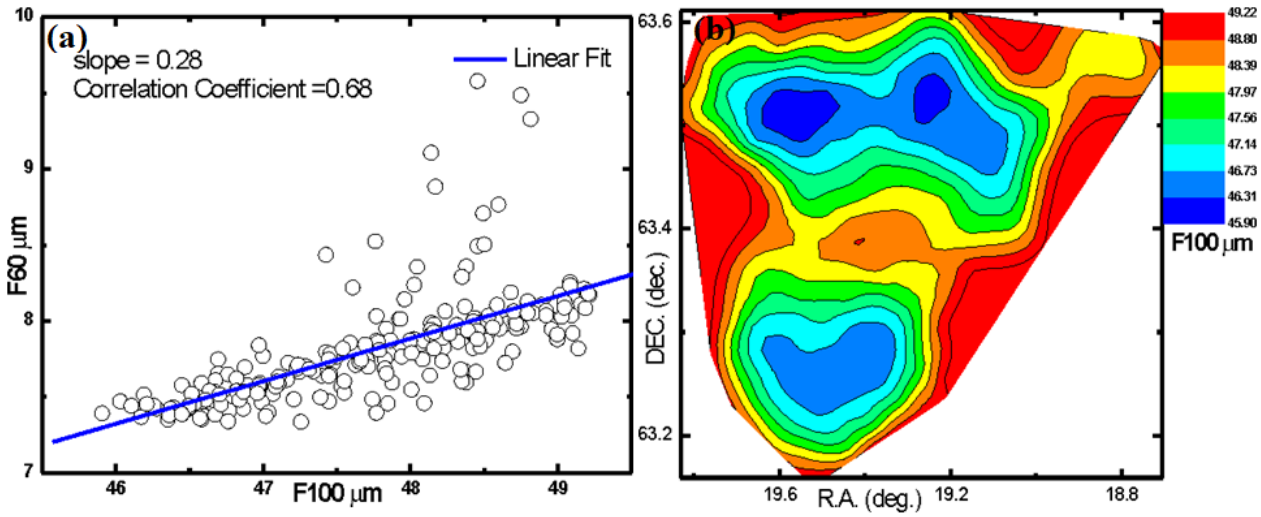

Fig. 3:(a) Flux at 60 μm (F60) versus flux at 100 μm (F100) scattered plot which suggest that the linearity between F60 and F100, the slope of the given distribution found to be with 0.28 error 0.02 and coefficient of determination nearly 0.68. Fig. (b) The flux density contour map of the inner region of the cavity at 100 μm. The contour levels and the color bars are shown.

4.2 Gaussian Plot of Temperature and Mass

We have plotted the Gaussian plot of dust color temperature and dust mass. The Gaussian center is found to be 23.76 K which is near to the average value of temperature the region i.e. 25.08 K. Here number of pixels corresponding to average value of temperature is maximum. The relatively lower value of temperature leads low value of error suggest that uniformity and consistency in temperature. The sharpness in curve represents dust color temperature of the pixels in the cavity region are found to be near to the average temperature. The graph between the number of the pixels and temperature is slightly positively skewed. Similarly we obtained the information about dust mass distribution. The Gaussian area of dust mass was found to be 2.10×10^{28} kg, whereas Gaussian center 4.06×10^{26} kg. The Gaussian average represents the most abundant pixel dust mass around the star CGCS201. The non-uniform (right skewed) distribution of dust mass shows that there is fluctuation in density which implies that the ISM grains are in the form of inhomogeneous distribution of ISM matter within region of interest.

4.3 Contour Plot of Mass and Temperature

The distribution of the Right ascension and Declination with the dust color temperature and dust mass has been plotted as shown in Fig. 5. The contour plot of Fig. 5 (a) and (b) shows the nearly inverse relationship between the mass and temperature.

The average dust mass inside the structure is found to be $(0.00024)M_{\odot}$. We found the minimum mass at the high temperature region. And mass is highly concentrated at the right side of the neck of the cavity structure.

The continuous distribution of the temperature with at given right ascension and declination is shown in the Fig. 5 (b). By using origin 8.0 the three dimensional plot has displayed. There is rise in temperature from violet to red color. The temperature has lies within the range 18.76 ± 3.16 K to 33.21 ± 4.07 K. There is nearly inverse relation between the mass distribution and temperature distribution at different pixel coordinate. We found the temperature is high at the intersecting points of cavity, which have high flux density.

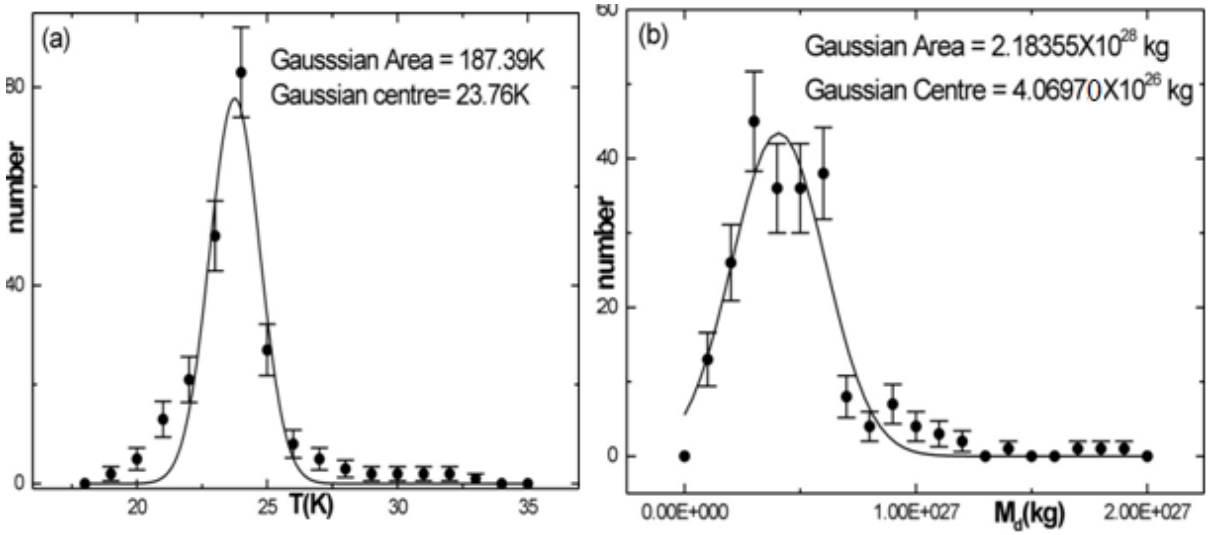

Fig. 4: (a), (b) The solid curve with error bar represents Gaussian plot of dust color temperature and mass respectively. Here error bar represents root square error in number of pixel corresponding calculated parameters.

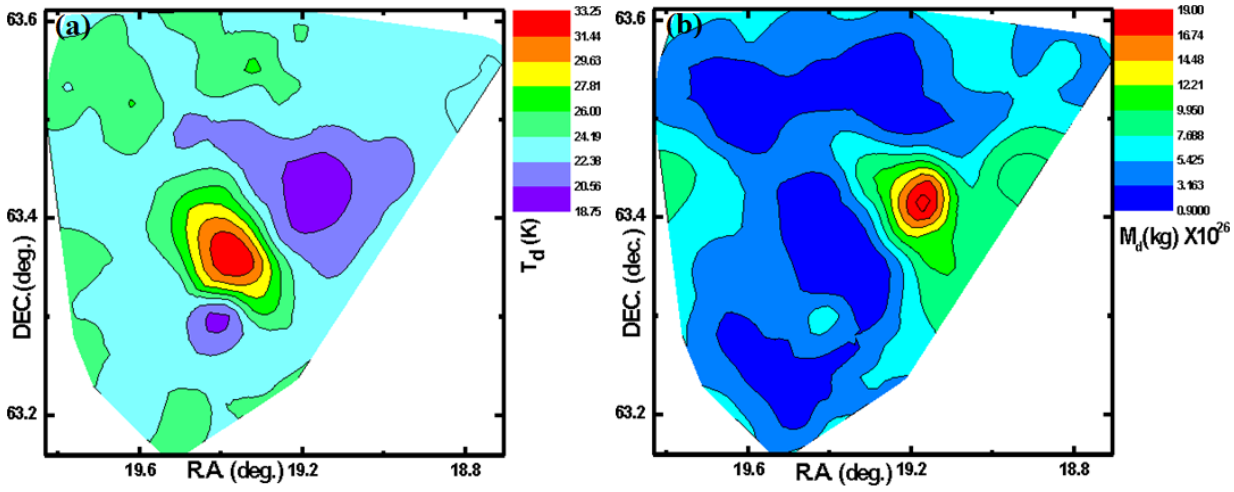

Fig. 5: (a)R.A./DEC.(J2000): $01^h\ 17^m\ 33{:}504^s$ $+63^0\ 22'\ 4.98''$ The contour plot of mass with respect to Right Ascension and Declination and (b) The contour plot of temperature with respect to right ascension and declination.

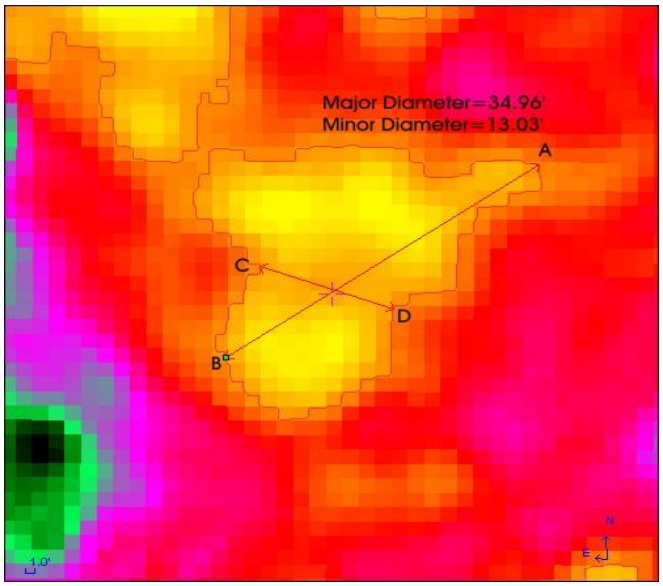

Fig. 6: Representation of extension (AB) and contraction (CD) of dust structure around IRAS 01142+6306.

4.4 Isolated cavity structure & inclination angle

We proceed a systematic search using FITS image from which we discovered two differently isolated cavity in 60 μm and 100 μm IRAS map around AGB star named as IRAS 01142+6306 or CGCS 201 having R.A./Dec.(J2000): 01^h 17^m 33:504^s $+63^0$ 22' 4.98''. We have used Aladinv2.5 to find the closed loop for region of interest. The closed loop having extension i.e. we called major diameter 34.96'(45.67 parsec) and contraction i.e. minor diameter 13.03'(17.02 parsec) was found using Aladinv2.5. The region of interest or ambient medium is sketched. The shape and contour of the loop depends upon the flux distribution around AGB star and contour level. Different color flux density shows variation physical parameters around the region of interest. Here diameter AB representing major diameter and CD is minor diameter interestingly maximum flux is found at their intersecting point. Hence from this observation we have major axis (a) = 45.67 pc, minor axis (b) = 17.02 pc and the value of intrinsic flatness q = 0.33 as suggested by Holmberg (1946) for oblate spheroid structure then using equation (13) inclination angle found to be 79.46°. The inclination angle of the core region greater than 70° suggesting edge-on appearance.

5. Conclusion

This work contributed following understanding.

- We studied (100 μm and 60 μm) IRAS survey using Virtual SkyView Observatory, SIMBAD and other platform. The maximum at R.A./Dec.J(2000): 01^h 17^m $28.69^s/63^0$ 21'32.6'', minimum at R.A./Dec. J(2000): 01^h 16^m $36.08^s/63^0$ 26' 5.5" average temperature of ambient ISM around AGB star is 33.21± 4.06 K, 18.76 ± 3.16 K, 25.08 K respectively. Maximum at J(2000) R.A./Dec.: 01^h 16^m $38.29^{sec}/$ 63^0, 24', 10.3''), minimum at J(2000)R.A./Dec: 01^h 18^m 25.69^s / 63^0 30' 24.8" and average mass of the surrounding pixels are 1.89×10^{27} kg (0.00094 $M_\odot$), 9.16×10^{25} kg (0.00005 $M_\odot$) and 4.73×10^{26} kg (0.00024$M_\odot$) respectively. Due to more temperature difference, we realized that star is in late AGB phase.

- Environment around IRAS 01142+6306 shows dust color temperature and dust mass of the structure which indicates a very good agreement with Gaussian distribution, and contour maps follows as expected trend slightly variation due to region affected by surrounding high pressure events. By using linear fitting between 60 μm and 100 μm we found slope 0.28(with Error 0.02) which gives average temperature and coefficient of determination 0.68 which is nearly 1 gives 68% best fit. This suggests that there is linearly change in flux density. The data scattered above the line is due to the rapid increase in flux at intersecting points of two diameters inside the contour map.
- The inclination angle of the core region of IRAS 01142+6306 was found to be79.46^{o}, suggesting edge-on appearance and size of the structure found to be 45.67 pc ×17.02 pc.

Acknowledgement

We acknowledge Strasbourg astronomical Data Center (CDS) and Sky View Virtual Observatory. One of the authors (LK) acknowledges department of physics Amrit Campus, Tribhuvan University, Nepal for all kinds of supports during this research work.

References

[1] D. P. Cox, The Three-Phase Interstellar Medium Revisited, Annu. Rev. Astron. Astrophys. 43 (2005, September) 337-385. doi.org/10.1146/annurev.astro.43.072103.150615.

[2] K. M. Ferriere, The interstellar environment of our galaxy, Reviews of Modern Physics 73(4) (2001) 1031.

[3] H. P. Gail, S. V. Zhukovska, P. Hoppe & M.Trieloff, Stardust from asymptotic giant branch stars, The Astrophysical Journal 698(2) (2009) 1136. doi.org/10.1088/0004-637X/698/2/1136.

[4] T. R. Bedding, A. J. Boothm & J. M. Davis, (Eds.). (2013), Fundamental Stellar Properties: The Interaction Between Observation and Theory: Proceedings of the 189th Symposium of the International Astronomical Union, Held at the Women's College, University of Sydney, Australia, 13–17 January 1997 (Vol. 189), Springer Science & Business Media.

[5] I. Iben, & A. Renzini,, Asymptotic giant branch evolution and beyond, Annual Review of Astronomy and Astrophysics 21(1) (1983) 271-342.

[6] B. Aryal, & R. Weinberger, A new large high latitude cone-like far-IR nebula, Astronomy & Astrophysics 448(1) (2006) 213. doi.org/10.1051/0004-6361:20042440.

[7] A. K. Jha, B. Aryal, & R. Weinberger, A study of dust color temperature and dust mass distributions of four far infrared loops. Revista Mexicana de Astronomía Astrofísica 53(2) (2017) 467-476.

[8] R. Guandalini, M. Busso, S. Ciprini, G. Silvestro, & P. Persi, Infrared photometry and evolution of mass- losing AGB stars-I. Carbon stars revisited. Astronomy & Astrophysics 445(3) (2006) 1069-1080. doi.org/10.1051/0004-6361:20053208.

[9] http://skyview.gsfc.nasa.gov/current/cgi/query.pl (2017).

[10] R. H. Hildebrand, The Determination of Cloud Masses and Dust Characteristics from Sub millimeter Thermal Emission, Journal of Royal Astronomical Society 24 (1983) 267-282.

[11] http://simbad.u-strasbg.fr/simbad/sim-fcoo (2017).

[12] S. L. Schnee, , N.A. Ridge, A. A. Goodman, G. L. Jason, A Complete Look at The Use of IRAS Emission Maps to Estimate Extinction and Dust Temperature, Astrophysical Journal 634 (2005) 442-450.

[13] X. Dupac, J. P. Bernard, N. Boudet, M. Giard, J. M. Lamarre, C. Mny, F. Pajot, , I. Ristorcelli, G. Serra, B. Stepnik, J.P. Torre, Inverse Temperature Dependence of the dust sub millimeter spectral index, Astronomy & Astrophysics 404 (2003) L11-L15. doi.org/10.1051/0004-6361:20030575.

[14] K.Young, T.G. Philips, G. R. Knapp, Circumstellar Shells resolved in IRAS Survey data II-Analysis, Astrophysical Journal 409 (1993) 725. doi.org/10.1086/172702.

[15] C. A. Beichman, G. Neugebauer, H. J. Habing, P. E. Clegg, T. J. Chester, Infrared Astronomical Satellite (IRAS) Catalogues and Atlases I: Explanatory Supplement. US Government Printing Office, Washington (1988).

[16] E. Holmberg, On the Apparent Diameters and the Orientation in Space of Extragalactic Nebulae Medd. Lund Astron. Obs. Ser. VI, (1946) 117.